

## Tracking Control of the Maximum Power Point (MPPT) In A Small Wind Turbine (SWT) For Isolated Residential Applications

David R. López Flores, José A. Pineda Gómez, Roberto Herrera S., Marcelino S. Alvarado.

Universidad Tecnológica de Chihuahua.

Dpto. de Mecatrónica y Energías Renovables.

Ave. Montes Americanos No. 9501 Sector 35

C.P. 31216 Chihuahua, Chih., México, Tel.: +52 (614) 4-32-20-00 ext. 105

José A. Duarte Moller\*

Centro de Investigación en Materiales Avanzados, S.C. Maestría en Energías Renovables

Ave. Miguel de Cervantes 120, Complejo Industrial, C.P. 31109, Chihuahua Chih., México

Tel.: +52 (614) 439 1100

*Abstract:* - This work shows the design, analysis, simulation and implementation of a tracking control Maximum Power Point (MPPT) in a Small Wind Turbine (SWT) with fixed angle  $\alpha$ . The MPPT controller extracts the maximum available kinetic energy of the wind  $V$ , which is converted to mechanical power  $P_m$  by the wind rotor shaft, followed by an electrical power  $P_e$ . Permanent Magnet Synchronous Generator, (PMSM), and a current three-phase rectifier alternating AC-DC, direct current, voltage  $V_r$ , generated converter is regulated by a reducer to DC-DC optimal load to maintain a deep cycle battery, using a Proportional Integral controller (PI) and equations relate  $V$ ,  $Mn$ ,  $V_r$  and angular velocity of the wind rotor  $W$  optimizing the output voltage  $V_r$  \* to maintain maximum energy extraction from the wind at any speed and load demand. A DC-DC boost converter with a PI controller and DC-AC inverter provides AC voltage with low harmonic distortion for residential applications.

*Key-Words:* - Tracking system control, MPPT, SWT

### 1 Introduction

Solar energy received by the planet earth is about 174.423 TW, of which an estimated 1 to 2 % is converted into kinetic energy (wind) due to wind generated by the impact of solar radiation on the surface of the land, which is an energy of between 1744.23 TW and 3488.46 TW<sup>1</sup>, surpassing by 28,859 to 57,718 times the national installed capacity for electricity generation in December 2009<sup>2</sup>. This represents a major breakthrough for the use of such renewable energy (wind) which does not pollute the environment, such as the use of fossil fuels like coal, oil and gas for electric power demand for the country. In the conversion of wind energy to electricity using wind rotors that catch the wind's kinetic energy and transform it into mechanical energy, which varies according to wind speed impacting the blades of the wind rotor. The resulting mechanical energy is converted to AC power through a generator PMSM, which are so this means that the DC-DC converter operates in open loop. Some studies focus on three-phase rectifier bridge to control the AC / DC<sup>3</sup> which is

commonly used in small wind turbines for residential, as they have high efficiency variable speed wind<sup>3</sup>. Betz limit that provides maximum efficiency (power coefficient  $C_p$ ) that can achieve a wind rotor is 59 % which is obtained by keeping an optimal point in the relative velocity edge (RRT, Tip Speed Ratio) for any speed Wind and load demand, and is a function of the wind rotor radius  $R$ ,  $W$  and  $V$ <sup>4</sup>. At this point, is the focus of some researchers, such as that presented by Md. Arifujjaman<sup>5</sup>, which provides optimal relationships between the wind speed, the angular velocity of the wind rotor and the duty cycle  $d$  of a DC-DC boost converter that is in turn connected to a single-phase DC-AC inverter, control of the wind rotor is regulated by a PI controller that compares the optimal speed  $W^*$  and  $W$  against the current speed and thus be hindering rotor axis by actuators, to reach optimal speeds maintaining the maximum  $C_p$ , and  $d$  is set to maintain a stable output of the inverter in CA, connected to the generator output to control PMSM angular velocity of the wind rotor, or by controlling a DC-DC converter that regulates the optimum load

a stabilizing system (batteries), so that the  $C_p$  is kept close to Betz limit<sup>6,7</sup>.

The system proposed in this research is shown in Figure 1, the MPPT control (DC-DC buck converter with input filter) is done by setting, for each wind speed there is an optimum voltage  $V$  and  $V_r^*$  which maintains the output current  $I_r^*$  necessary to charge the battery bank (stabilizer) and due to the electromagnetic field generated by  $I_r^*$  in the rotor, this opposes the magnetic field PMSM motor stator,

thereby reducing the speed  $W$ , maintaining the relationship  $TSR$  and  $C_p$  in optimal values of 6 to 8 and from 0.4 to 0.5 respectively for small wind turbines<sup>8</sup>.

A DC-DC boost converter is connected to a 24 V battery bank to raise the voltage to 170 V, entering the DC-AC inverter with SPWM shooting technique, generating a voltage of 120 V<sub>rms</sub> with low harmonic distortion due to filter output.

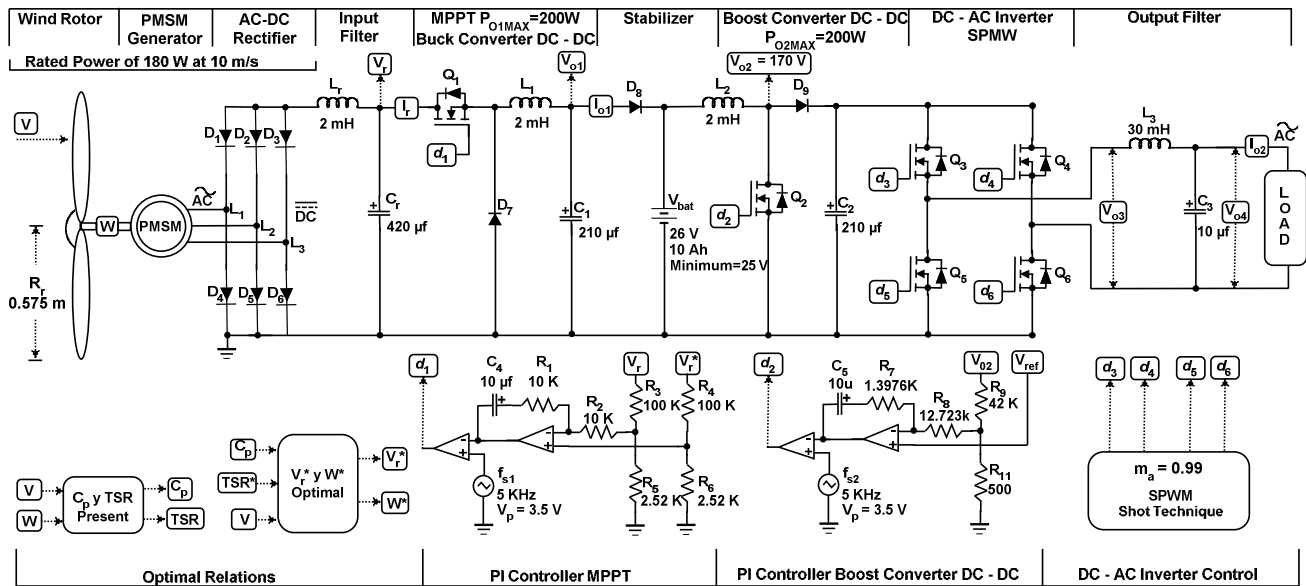


Figure 1. Proposed MPPT control system in a wind turbine.

## 2 Problem Formulation

This section analyzes the MPPT control strategy based on optimal relationships between wind speed and voltage AC-DC rectifier, in order to establish the proportional integral controller design of the MPPT. Furthermore, the analysis and design of DC-DC boost converter that conditions a bus voltage of 24 V to 170 V in DC for the DC-AC inverter, which delivers 120 V AC with low harmonic distortion (THD) due to technical shots of pulse width modulation sine (SPWM) and the LC filter.

### 2.1 Strategy of MPPT.

Figure 2 shows the maximum electrical power curve  $P_e$  SWT turbine for different wind velocities, it can be seen that there is a line joining the optimal points of electrical power as a result of the product  $I_r^* \times V_r^*$ , indicating that for each wind speed  $V$  exists an optimum value of the rectifier output voltage  $V_r^*$ , resulting in maximum power coefficient and relative velocity of the wind turbine tip. MPPT controller seeks to follow the optimal points of the maximum power curve according to Figure 2, using relations

between the wind speed and voltage of the rectifier AC / DC uncontrolled six pulses per cycle.

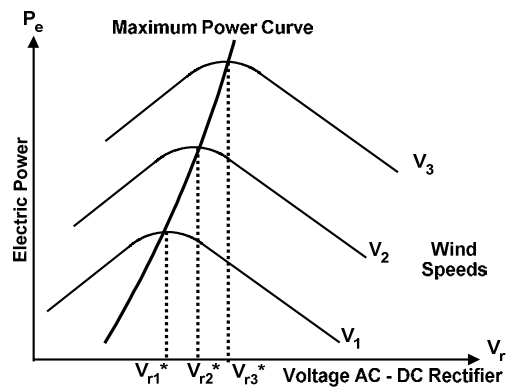


Figure 2. Maximum electrical power curve.

### 2.2 Optimal relations

A wind turbine captures the kinetic energy due to wind through the blades, turning some of this energy into mechanical energy due to the Betz limit, which is given by the following relation<sup>9</sup>:

$$P_m = \frac{1}{2} \rho A_r C_p(TSR, \alpha) V^3 \quad (1)$$

Where  $\rho$  is the density of air density,  $A_r$  wind rotor area of the power coefficient  $C_p$  as a function of tip speed and angle of attack (vacated in the case of the turbine *SWT*). *TSR* tip speed is determined by using equation 2<sup>9</sup>.

$$TSR = \lambda = \frac{R_r W}{V} \quad (2)$$

here  $r$  is the radius of the wind turbine rotor. Whereas the rake angle is fixed and a wind turbine *SWT*, the power coefficient is a function only of *TSR* and can be estimated according to Equation 3<sup>5</sup>.

$$C_p = C_1 \lambda^4 - C_2 \lambda^3 + C_3 \lambda^2 - C_4 \lambda + C_5 \quad (3)$$

And:

$$C_1 = 0.00044, C_2 = 0.012, C_3 = 0.097, C_4 = 0.2 \\ C_5 = 0.11$$

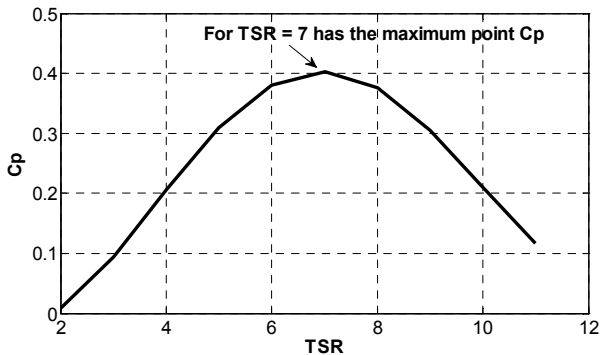


Figure 3. Power coefficient based on *TSR*.

Figure 3 shows the relationship between the power coefficient and the tip speed match graphed result of equation 1 and 2 where it is remarkable that for a given speed  $V$  and  $W$  is a maximum power coefficient, however, the normal operation of a turbine without control is such that the more wind speed, the angular velocity increases in greater proportion than  $V$ , as a result of this a departure from the optimum point of the power coefficient, it states that it is necessary to have a controller with optimal relations of  $V$ ,  $W$ , and  $V_r$  determine the maximum extraction power of the wind turbine.

If the term of  $C_p$  does not limit the equation 1, we obtain mechanical power nearly doubled, however, the parameter  $C_p$  leads us to conclude that the maximum efficiency that can have a wind turbine is 59 %.

The mechanical power is converted to electrical power through the *PMSM* motor, generating a voltage from line to line effectively given by equation 4.

$$V_{gll} = \frac{1}{\sqrt{2}} K_v W \sin(Wt) \quad (4)$$

Where  $K_v$  is a constant that can be obtained by experimental measurements according to equation 5:

$$K_v = \frac{\sqrt{2} \times V_{gll}}{W} \cong 0.69 \quad (5)$$

And  $t$  the generator frequency according to the number of poles of the generator  $N_p = 12$  and  $W$ .

$$t = \left( W N_p / 2 \right)^{-1} \quad (6)$$

The voltage generator is rectified and converted to *CD* by *AC-DC* rectifier, and is a function of  $V_{gll}$  and voltage  $V_D$  of the rectifier diodes (Equation 7).

$$V_r = \frac{3\sqrt{2}}{\pi} V_{gll} - 2V_D \quad (7)$$

$W^*$  The optimal speed for a wind turbine *SWT* is given by Equation 8<sup>5</sup>

$$W^* = 3 \sqrt{\frac{P_m}{K_{opt}}} \quad (8)$$

$$\text{Where: } K_{opt} = \frac{1}{2} \rho A_r C_p(TSR, \alpha) \left( \frac{R_r}{\lambda} \right)^3 \quad (9)$$

Assuming a relative velocity optimum  $TSR = 7$  for any wind speed  $V$  and introducing the equation 8 in equation 4 provides the relationship of the optimal generator voltage for a given wind speed.

$$V_{gll}^* = \frac{1}{\sqrt{2}} K_v 3 \sqrt{\frac{P_m}{K_{opt}}} \sin \left( 3 \sqrt{\frac{P_m}{K_{opt}}} t \right) \quad (10)$$

Here:

$$K_{opt} = \frac{1}{2} \rho A_r C_p(TSR=7) \left( \frac{R_r}{7} \right)^3 \quad (11)$$

$$P_m = \frac{1}{2} \rho A_r C_p(TSR=7) V^3 \quad (12)$$

Finally, by substituting equation 10 into equation 7 we obtain an optimum ratio between the voltage of the rectifier and the wind speed through  $V_{gll}^*$ .

$$V_r^* = \frac{3\sqrt{2}}{\pi} V_{gll}^* - 2V_D \quad (13)$$

Since *TSR* is set to an optimal point 7 for any value of *V* according to Figure 3, it is possible to determine the angular velocity *W* using equation 2 and the power coefficient according to equation 3, these parameters are essential for determining  $M_w$  and  $k_{opt}$  in equation 9, which implies that it is only necessary sensing wind speed *V* to determine the optimum voltage  $V_r^*$  which should reach the *AC-DC* rectifier to maintain the maximum possible power up on the wind turbine (Fig. 2).

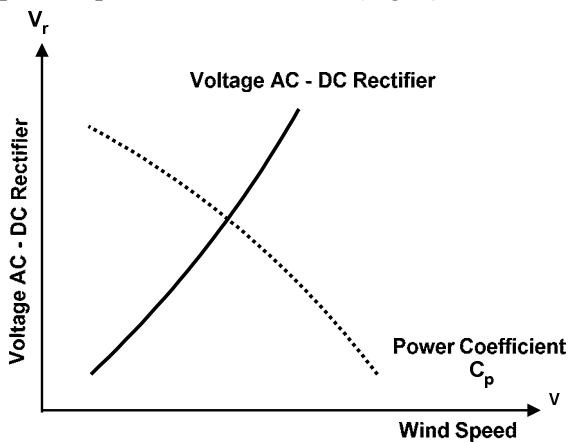


Figure 4. Power coefficient based on  $V_r$ .

### 2.3. PI controller MPPT.

From Figure 1, if the voltage of the rectifier  $V_r$  is not manageable voltage that we would grow while the wind speed increase, causing a decrease in the power coefficient  $C_p$  due to increased angular speed *W* and in turn increased *TSR* relative speed, this can be seen in Figure 4.

To maintain the voltage  $V_r$  in an optimum point controlled according to equation 13, interconnects

the output of the *AC-DC* rectifier to a *DC-DC* buck converter with  $L_r, C_r$  input filter that reduces the ripple voltage and current caused by the switching of the switch  $Q_1$  (see Figure 1).

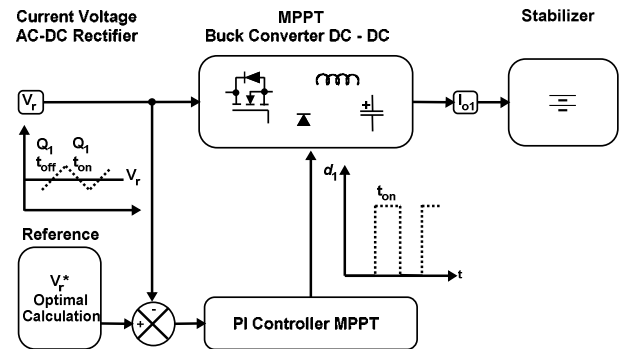


Figure 5. PI controller MPPT.

The *DC-DC* buck converter is controlled by a proportional integral *PI* regulator (see Figure 5), where the feedback is from the voltage  $V_r$ , since it is the parameter to be controlled, this voltage is compared with the reference voltage  $V_r^*$  by equation 13, so that if the voltage of the rectifier  $V_r$  exceeds the reference voltage  $V_r^*$ , the *PI* controller generates an increase in the duration on  $Q_1$  (increased duty cycle  $d_1$ ) until the voltage  $V_r$  is set equal with  $V_r^*$ , that due to increased demand by the drive current, which causes the decrease of  $V_r$ . Otherwise the *PI* controller decreases the on time of  $Q_1$  (decreased  $d_1$ ) until  $V_r$  and  $V_r^*$  reach, so the driver constantly maintains optimal value  $V_r$  and  $V_r^*$  and the same according to equation 13, and as a result this keeps the maximum power coefficient  $C_p$ , moreover, that the output current of the converter  $I_{ol}$  always maintains its maximum load to the battery bank to any wind speed and load demand by the *DC-AC* inverter.

*MPPT* system response has open loop delay times *L* is not greater than 40 ms and rise time *T* not greater than 50 ms (see Figure 6), from this stage, applying the rules of Ziegler-Nichols tuning<sup>10</sup> approximate the constants of the *PI* controller, resulting in integration time  $T_i = 0.1$  s and a proportional constant  $K_p = 1$ .

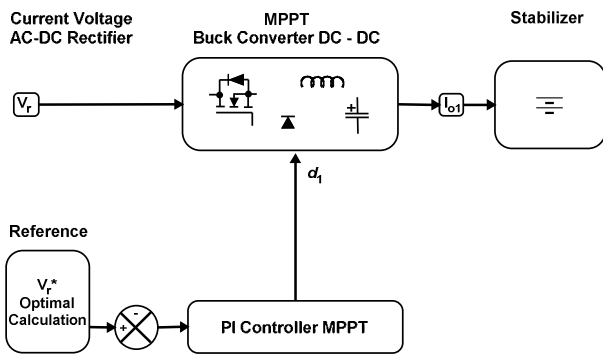
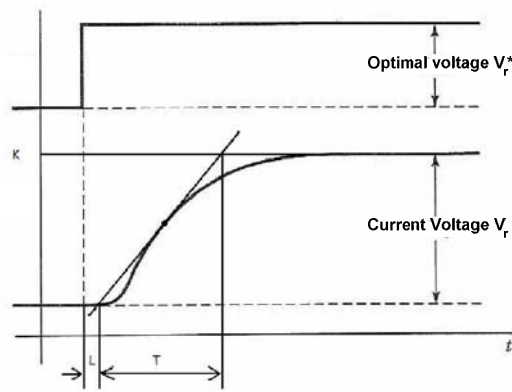


Figure 6. Open loop response of MPPT.

### 2.4 DC-AC inverter and DC-DC boost converter.

A DC-DC Boost Converter in voltage mode controlled by a PI controller (see Figure 7) is necessary to condition and stabilize the voltage of the battery bank to the input voltage bus ( $V_{o2} = 170$  V) DC-AC Inverter.

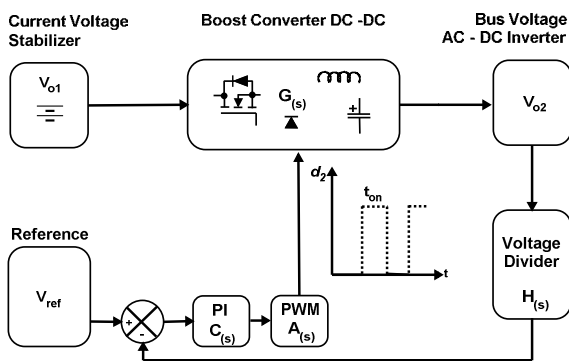


Figure 7. DC-DC boost converter in voltage mode.

Considering that the converter operates in continuous mode of driving the relationship between the output voltage  $V_{o2}$  and the duty cycle  $d_2$  (transfer function  $G(s)$ ) is given by the following equation <sup>11</sup>:

$$\frac{V_{o2}}{d_2} = \frac{V_i}{(1-D)^2} \frac{\left(1 + \frac{s}{W_{Z1}}\right) \left(1 - \frac{s}{W_{Z2}}\right)}{1 + \frac{s}{W_o Q} + \frac{s^2}{W_o^2}} \quad (14)$$

Where:

$$W_{Z2} = \left( (1-d_2)^2 (R - R_L) \right) / L_2 \quad (15)$$

$$W_{Z1} = 1 / (ESR * C_2) \quad (16)$$

$$W_o = \sqrt{\left( R_L + (1-d_2)^2 R \right) / R} / \left( \sqrt{L_2 C_2} \right) \quad (17)$$

$$Q = W_o / \left( (R_L/L) + (1/(C_2(R+ESR))) \right) \quad (18)$$

and the inductor resistance  $RL$   $L_2$ , internal resistance  $ESR$  of the capacitor  $C_2$ , with values of  $0.12 \Omega$  and  $0. \Omega$  respectively.

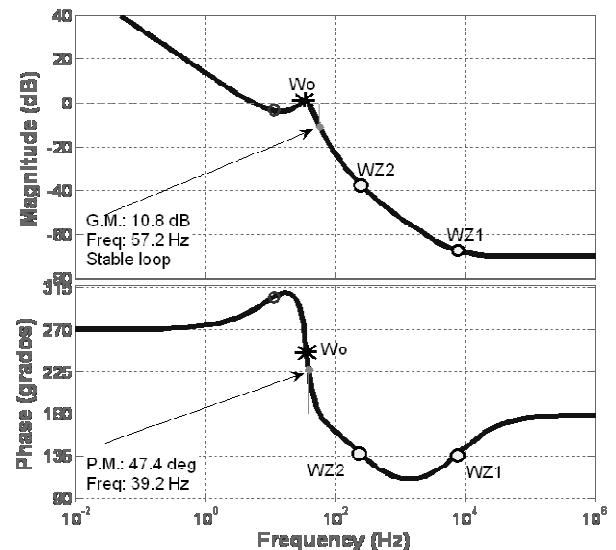


Figure 8. Bode plots of gain and phase DC-DC boost converter in closed loop.

Steady state design parameters and taking as according to figure 1, the choice of  $C_2$  is  $210 \mu F$  with an  $ESR$  of  $0.1 \Omega$  and  $L_2$  of  $2 \text{ mH}$  with  $RL = 0.12 \Omega$ , if the converter operates at maximum power load output is equivalent to  $R \approx 145 \Omega$  to a  $d_2 \approx 85$

%. Following the design of the converter to calculate the *PI* controller takes into account the Nyquist stability criteria (MG margin of at least -6 dB crossing of phase by 180° and a phase margin between *MF* 30° and 60° to the crossing of the gain from 0 dB) in the frequency domain<sup>11</sup>, moreover, that the new crossing of the gain from 0 dB is at 1/6 of the resonant frequency  $W_o \approx 236$  Hz with the order to minimize loss caused by the zero-phase minimum-phase (Eq. 15). Resulting in  $T_i = C_3R_7 = 0.0139$  s = 0.1098  $K_p = R_7/R_8$ . Using *MATLAB* the Bode plot gain and phase with the *PI* controller can be seen in Figure 8, which shows that meet the stability criteria described. The transfer functions of the controller  $C(s)$  and *PI*, the sensor  $H(s)$  (voltage divider) and the pulse width modulator  $A(s)$  (*PWM*) are indicated in the following equations:

$$C(s) = (K_p s + K_p / T_i) / s \tag{19}$$

$$C(s) = (0.1098s + 7.89) / s \tag{20}$$

$$H(s) = V_{o2} R_{11} / (R_9 + R_{11}) = 0.01176 \tag{21}$$

$$A(s) = 1/V_p = 0.2857 \tag{21}$$

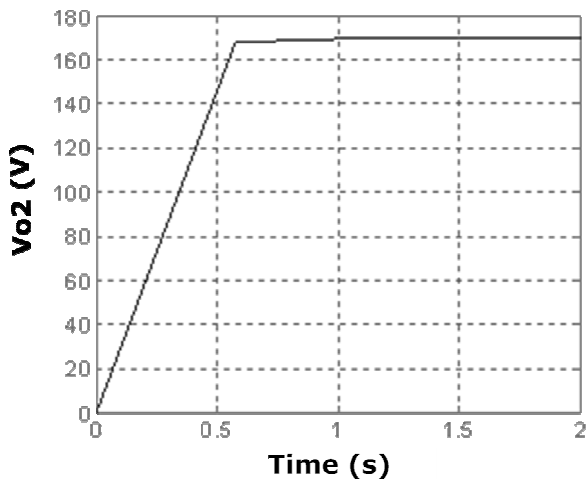


Figure 9. Step response of *DC-DC* boost converter in closed loop.

Figure 9 shows the step response of *DC-DC* boost converter in voltage mode controlled by a *PI* controller, which reaches the final value ( $V_{o2} = 170$  V) in a time of no more than 1 second, due to low bandwidth of 39.2 Hz selected to avoid the effect of minimum-phase zero.

The technique of firing pulse width modulated sinusoidal (*SPWM*) is applied to activate the *DC-AC* inverter<sup>12</sup>, which is shown in Figure 10. The technique consists in comparing a sinusoidal control signal  $V_{Control}$  respect a  $V_{carrier}$  against a triangular carrier, the result of the comparison generates a train of modulated pulses that are injected into the gates of the switching devices  $Q_3, Q_4, Q_5$  and  $Q_6$ , which when become activated bus inverter input voltage to a voltage of +170 V to bipolar -170 V, with high harmonic distortion *THD*.

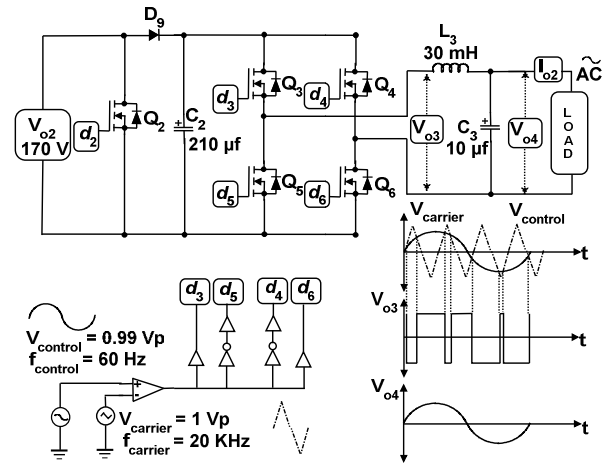


Figure 10. *DC-AC* inverter controlled by *SPWM* technique.

*THD* factor to decrease and increase the quality of output waveforms of the inverter, the fundamental frequency is extracted by an *LC* filter designed for a cutoff frequency  $f_c = 290$  Hz which is suitable because it is less than the frequency of the carrier signal  $f_{carrier} = 5$  kHz, resulting  $L_3 = 30$  mH and  $C_3 = 10$  µf. The magnitude of the fundamental signal depends on the relationship,  $V_{fundamental} = V_{O4} = (m_a \times V_{o2}) / \sqrt{2}$ , where  $m$  is called the modulation index and is given by the  $V_{control} / V_{carrier}$ .

### 3 Simulation and Experimental Results

For the implementation of the wind turbine and *DC-DC* buck converter modules are used *Lab-Volt*. For the boost converter and *DC-AC* inverter is used a 2 KW inverter power input, 24 V and 120 V output sine wave with low harmonic distortion. The *MPPT* control circuit is integrated development with the *SG3524*, the architecture contains an error amplifier for the implementation of the *IP*, in addition, the *PWM* circuit. The calculation of  $V_r^*$  is not carried out in an experimental simulation is taken from the reference value  $V_r^*$  and adjusted with a knob at the

entrance to the positive terminal of the *PI* controller *MPPT*, this, before establishing a speed of wind in the *Lab-Volt* module, therefore it is not possible to perform experimental tests of a speed change to another to analyze the controller's response time, but in this simulation procedure is possible.

According to Figure 1, the circuit simulation is implemented in *MISP* (power simulation program) taking into account the parameters indicated in Figures 1 and 7.

Due to high electrical currents that can withstand the *Lab-Volt* modules was established as a wind speed limit at 7m / s, for which in Figure 11 shows the results of  $V_r * V_r$ ,  $I_r$  and  $C_p$  simulation considering a load connected to the inverter of 60W, wherein the power coefficient is maintained at a value greater than 0.4 and the optimum value of the rectifier voltage is reached, as determined in Section I.

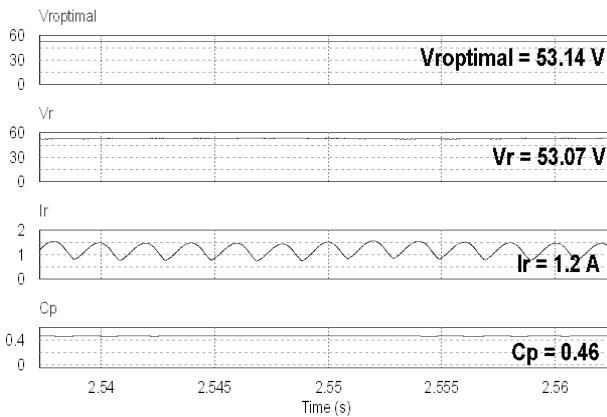


Figure 11. Simulation results of  $V_r * V_r$ ,  $I_r$  and  $C_p$ , for  $V = 7\text{m / s}$ .

In Figure 12 appears the experimental results for a wind speed of 7 m / s  $V_r$  and  $I_r$ , in which there is a voltage of 52.5 V and a current of 1.27 A, very similar to the simulation results. Figure 13 and 14 shows the experimental and simulation results, respectively, of the step response ( $V = 7\text{ m / s}$ ) system for  $V_r$  and  $I_r$ , in which we see that the time that stabilizes the 53V is approximately 1s.

For a load of 60 W, in Figure 15 and 16 shows the experimental and simulation results, respectively, of voltage and current of the inverter output *LC* filter, and  $m = 0.99$ , in which a good quality can be seen in waveform and magnitude values approximately equal.

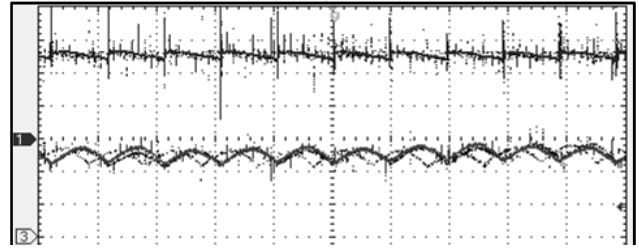


Figure 12. Experimental results of  $V_r$  (Ch1: 20 V / div, 2 ms / DIV) and  $I_r$  (Ch3: 500 mA / div, 2 ms / DIV).

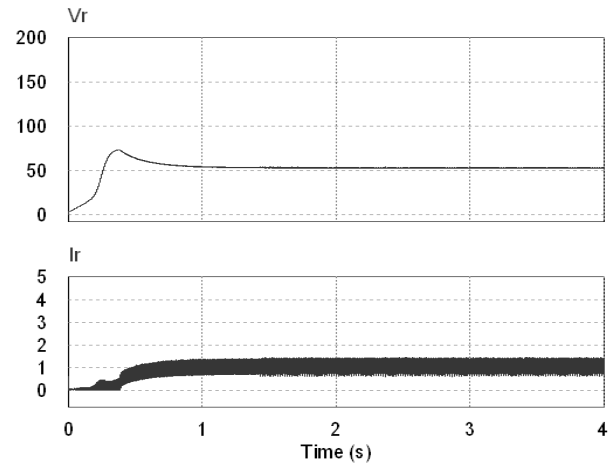


Figure 13. Simulation results of  $V_r$  and  $I_r$  with a step of  $V = 7\text{m / s}$ .

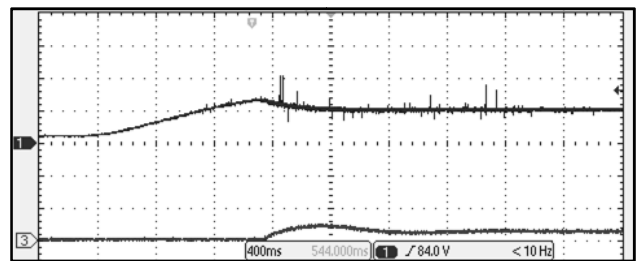


Figure 14. Experimental results of  $V_r$  (Ch1: 50 V / div, 400 ms / DIV) and  $I_r$  (Ch3: 5 A / div, 400 ms / DIV), with a step of  $V = 7\text{m / s}$ .

The response of *PI* controller *MPPT* simulation to changes in wind speed of 5 m / s to 7 m / s can be seen in Figure 17 for  $V_r * V_r$  and  $C_p$ , which is seen as transitioning the  $C_p$  and  $V_r$  to stabilize at their optimum values.

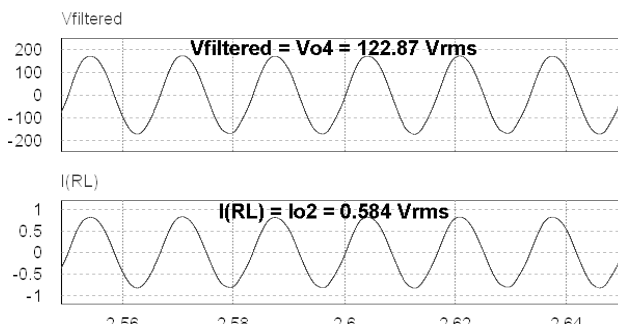


Figure 15. Simulation results of voltage and output current of the inverter to a power of 60W.

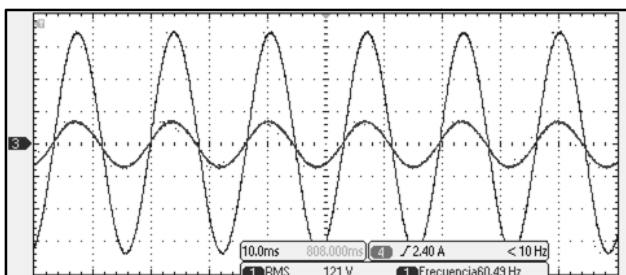


Figure 16. Experimental results of voltage (Ch1: 50 V / div, 10 ms / div) and current (Ch3: 1 A / div, 10 ms / DIV) output of the inverter.

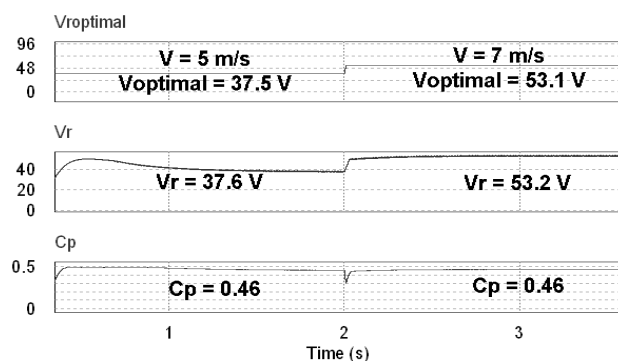


Figure 17. Simulation results of  $V_r * V_r$  and  $C_p$  for wind speed transitions.

## 4 Conclusions

Is shown in this simulation, an applied research, design and implementation of a tracking control system of the maximum power point of a small isolated wind turbine applications to conventional electricity network, also design and simulation of a boost converter  $CD -CD$  and  $DC-AC$  inverter with high quality in its output waveforms for the power conditioning from the stabilizer to the load. The experimental and simulation results were as expected, thus validating the theory and methodology of system control  $MPPT$  wind turbine.

The relationship between the rectifier voltage and wind speed according to equation 13, support the value of reference to follow for the PI controller  $MPPT$  and thus maximum power coefficient of the wind rotor to wind speeds and load variables.

$PI$  controller of the boost converter  $DC-DC$  is designed to compensate before the phase loss due to the minimum-phase zero the system presents, however, this approach limits the compensation bandwidth to 39.2Hz giving response times to 1 seconds (see Figure 8).

## References

- [1] Danish Wind Industry Association, “*De Donde Viene la Energía Eólica*”. Disponible en: <http://guidedtour.windpower.org/es/tour/wres/index.htm>.
- [2] Secretaria de Energía, “*Prospectiva del Sector Eléctrico 2010-2025*”. Disponible en: [http://www.energia.gob.mx/res/1825/SECTOR\\_ELECTRICO.pdf](http://www.energia.gob.mx/res/1825/SECTOR_ELECTRICO.pdf)
- [3] M. Hilmy, M. El-Nemr, M. Youssef, “A Less Sensor Control Method for Standalone Small Wind Energy Using Permanent Magnet Synchronous Generator”, IEEE APEC’11, Conference Publications, pp. 1968 – 1974. Abril 2011.
- [4] J.F. Manwell, J.G. McGowan, A.L. Rogers, “*Wind Energy Explained*”, John Wiley & Sons Ltd, 2002.
- [5] Md. Arifujjaman, “Modeling, Simulation and Control of Grid Connected Permanent Magnet Generator (PMG)-based Small Wind Energy Conversion System” IEEE EPEC’10, Conference Publications, pp. 1-6. Agosto 2010.
- [6] H. Xu, J. Hui, D. WU, W. Yan, “*Implementation of MPPT for PMSG-Based Small-Scale Wind Turbine*”, IEEE ICIEA’09, Conference Publications, pp. 1291-1295, Mayo 2009.
- [7] D. Oliveira, G. Sousa, A. Rangel, D. Queiroz, L. Santos, L. Fontenele, P. Bezerra, “*Low Cost and High Efficiency Static Converter For Small Wind Systems*”, IEEE COBEP’09,



Conference Publications, pp. 972 – 977,  
Octubre 2009.

- [8] M. Abdel-Salam, a. Ahmed, M. Abdel-Sater, “Maximum Power Point Tracking for Variable Speed Grid Connected Small Wind Turbine”, IEEE ENERGYCON’10, Conference Publications, pp. 600-605, Diciembre 2010.
- [9] G. Putrus, M. Narayana, M. Jovanovic, P. Sing, “Maximum Power Point Tracking For Variable-Speed Fixed-Pitch Small Wind Turbines”.
- [10] K. Ogata, “*Ingeniería de Control Moderna*”, Tercera Edición, Publicada por Prentice-Hall Hispanoamericana, 1998.
- [11] D. López, A. Lizárraga, J. Durán, “Diseño y Consideraciones de un Lazo de Compensación para el Convertidor Tipo Boost (Elevador) Cd-Cd Controlado en Modo de Voltaje”, ELECTRO’04, Conferencia, Octubre 2004.
- [12] N. Mohan, “*Electrónica de Potencia, Convertidores, Aplicaciones y Diseño*”, Tercera Edición, Publicada por Mc. Graw Hill, 2009.